

VIP Very Important Paper

# Carbon-Free Cathode Materials for Li–O<sub>2</sub> Batteries

Deqing Cao,<sup>[a]</sup> Shuaishuai Zhang,<sup>[a]</sup> Fengjiao Yu,<sup>[a]</sup> Yuping Wu,<sup>\*[a]</sup> and Yuhui Chen<sup>\*[a]</sup>

Rechargeable lithium-oxygen batteries, especially the nonaqueous lithium-oxygen batteries have attracted much attention in recent years due to their high energy densities. However, few critical challenges remain to be overcome, including the low round-trip efficiency, high charge overpotential, poor cycling performance, decomposition of electrolyte, and instability of the carbon-based electrode. Among these, the instability of the

carbon-based electrode is one of the major problems that hindered the practical application of the Li–O<sub>2</sub> batteries. Much work has been done to solve this problem and there are two widely-applied strategies: modification of carbon and designing a “carbon-free” cathode. In this review, we will introduce recent achievements of both strategies.

## 1. Introduction

Rechargeable lithium ion batteries offer great convenience for people in various aspects, particularly with regard to portable electronic devices, battery-power electrical vehicles and energy storage. Nevertheless, the maximum achievable specific energy of lithium ion battery is 250 Wh kg<sup>-1</sup>, limiting their widespread application in the field that demands high energy density battery.<sup>[1]</sup> Therefore, the most feasible approach is to seek alternative battery systems. Lithium-air battery has attracted much interest because of its high theoretical specific energy (3500 Wh kg<sup>-1</sup> based on cathode reaction: O<sub>2</sub>+2Li<sup>+</sup>+2e<sup>-</sup>→Li<sub>2</sub>O<sub>2</sub>). However, the H<sub>2</sub>O and CO<sub>2</sub> from air cause some undesirable reactions. Particularly, the influence of H<sub>2</sub>O on discharge and charge process is complicated and not well understood yet.<sup>[2,3]</sup> To move forward step by step, researchers replace air with pure O<sub>2</sub> to prevent these complicated side-reactions. Therefore, lithium-air batteries are usually called the lithium-oxygen (Li–O<sub>2</sub>) batteries.

Li–O<sub>2</sub> batteries are classified into four types according to electrolytes in the cells: nonaqueous,<sup>[4]</sup> aqueous,<sup>[5,6]</sup> solid-state<sup>[7]</sup> and hybrid<sup>[8,9]</sup> (Figure 1). Research interests mainly focus on the nonaqueous Li–O<sub>2</sub> battery due to its relatively simple structure. A nonaqueous Li–O<sub>2</sub> battery consists of a porous cathode, a metallic Li anode and nonaqueous electrolyte in between (Figure 1a). The aqueous system<sup>[5,6]</sup> offers a large ionic conductivity of electrolyte, the discharge process of which is based on a 4e<sup>-</sup> oxygen reduction reaction (ORR). (Figure 1b). ORR has been extensively investigated in fuel cells and lots of catalysts have been developed. Nevertheless, the use of aqueous system is limited due to the inevitable side-reactions of metallic lithium anode in water. A stable Li-ion conductive layer such as solid-

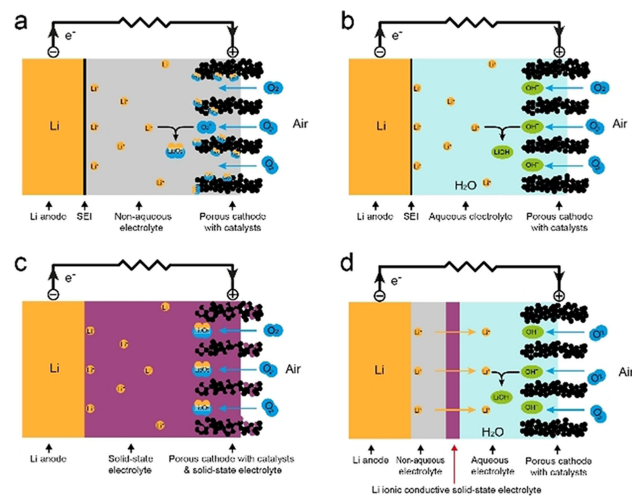


**Figure 1.** Schematics of four types of Li–O<sub>2</sub> cells. (a) non-aqueous cell; (b) aqueous cell; (c) solid-state Li–O<sub>2</sub> cell and (d) hybrid cells using a solid-state electrolyte to protect Li anode from side-reactions with H<sub>2</sub>O.

state electrolyte has to be applied to protect the Li anode, but some solid-state electrolytes such as Li<sub>1.4</sub>Al<sub>0.4</sub>Ti<sub>1.6</sub>(PO<sub>4</sub>)<sub>3</sub> (LATP) react with Li and cause compatibility problems. In 1987, Semkow et al.<sup>[7a]</sup> first built a solid-state Li-air battery but at a high temperature. In 2010, Kumar et al.<sup>[7b]</sup> reported a solid-state Li-air battery where ceramics, Li<sub>1.5</sub>Al<sub>0.5</sub>Ge<sub>1.5</sub>(PO<sub>4</sub>)<sub>3</sub> (LAGP), and PEO-based polymer electrolytes were used (Figure 1c). The restricted Li ionic conductivity of the solid-state electrolyte and challenges of the interface have to be addressed. To avoid the poor solid-solid contact and side-reactions between Li anode and solid-state electrolyte, a buffer layer such as nonaqueous electrolyte was introduced in between. Zhou and co-workers proposed the concept of Li–O<sub>2</sub> cells using hybrid electrolyte,<sup>[8,9]</sup> which integrated ORR in an aqueous solution and a Li anode in a nonaqueous electrolyte. But the cost of solid-state electrolyte is a concern. (Figure 1d)

In this review, we focus on the nonaqueous Li–O<sub>2</sub> batteries, which was proposed in 1996 by Abraham et al.<sup>[4]</sup> The cell operates at room temperature and the discharging process is mainly based on a 2e<sup>-</sup> ORR. The charging process is a 2e<sup>-</sup>

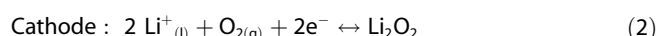
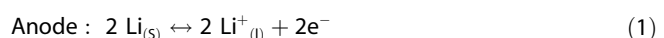
[a] D. Cao, S. Zhang, F. Yu, Prof. Y. Wu, Prof. Y. Chen

State Key Laboratory of Materials-oriented Chemical Engineering  
School of Energy Science and Engineering  
Nanjing Tech University  
Nanjing, Jiangsu, 211816 China  
E-mail: wuyp@njtech.edu.cn  
cheny@njtech.edu.cn

An invited contribution to a Special Collection dedicated to Metal-Air Batteries



oxygen evolution reaction (OER) based on  $\text{Li}_2\text{O}_2$  decomposition. Giordani et al.<sup>[10]</sup> demonstrated a molten salt  $\text{Li}-\text{O}_2$  cell using  $\text{LiNO}_3-\text{KNO}_3$  eutectic as electrolyte at 150 °C. Because the high temperature changes the thermodynamics of the reactions, the discharge reaction would be different and  $\text{Li}_2\text{O}_2$  might not be the only energy favorable products. For instance, very recently, Nazar and co-workers<sup>[11]</sup> demonstrated that  $\text{Li}_2\text{O}$  formed as a final discharge product in a  $\text{Li}-\text{O}_2$  cell using  $\text{LiNO}_3-\text{KNO}_3$  eutectic electrolyte at 150 °C. In this review, we mainly focus on the room-temperature  $\text{Li}-\text{O}_2$  cells. The main reactions involved are described below [Eq. (1) and (2)]:



Recently, Liu et al.<sup>[12]</sup> demonstrated a  $4\text{e}^-$  reversible reaction of forming and decomposing  $\text{LiOH}$  in the presence of  $\text{H}_2\text{O}$  and  $\text{LiI}$ . A  $1\text{e}^-$  reversible reaction forming/decomposing  $\text{LiO}_2$  was also demonstrated.<sup>[13]</sup> Here we focus on the  $2\text{e}^-$  reduction of  $\text{O}_2$  to form  $\text{Li}_2\text{O}_2$ .

The porous cathodes provide a conducting substrate as well as the accommodation for the solid-state discharge products ( $\text{Li}_2\text{O}_2$ ). Carbon has been widely used as electrode material in  $\text{Li}-\text{O}_2$  batteries, because of its high conductivity and large surface area. However, several studies have shown side-reactions of carbon occurred both in discharging and charging process.<sup>[14]</sup> Very recently, Peng and coworkers summarized the reaction mechanisms on the electrode-electrolyte interface,

including the typical side-reactions and their influence.<sup>[15]</sup> Reduced oxygen species, like superoxide and peroxide species, could attack carbon and form by-products. McCloskey et al.<sup>[14]</sup> first reported that carbon reacts with  $\text{Li}_2\text{O}_2$  on discharge. [Eq. (3) and (4)]



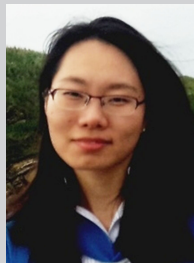
Gallant et al. agreed on the reaction between  $\text{Li}_2\text{O}_2$  and carbon.<sup>[16,17]</sup> However, Xu et al. and Ottakam Thotiyil et al. found little reaction take place between  $\text{Li}_2\text{O}_2$  and carbon on discharge.<sup>[18,19]</sup> Ottakam Thotiyil et al.<sup>[19]</sup> demonstrated that carbon decomposed to  $\text{CO}_2$  in the presence of  $\text{Li}_2\text{O}_2$  on charge, particularly at a potential over 3.5 V (vs.  $\text{Li}^+/\text{Li}$ ). Later, Zakharchenko et al.<sup>[20]</sup> claimed that the defects of carbon, such as epoxy groups on carbon lead to more side-reactions with superoxide radicals. Very recently, singlet oxygen ( ${}^1\text{O}_2$ ), a very reactive species, was identified in metal- $\text{O}_2$  cells.<sup>[21]</sup> Freunberger and coworkers<sup>[21a]</sup> showed the presence of  ${}^1\text{O}_2$  formed during discharge and it accounts for the majority of side reaction products and the highly reactive singlet oxygen may also react with carbon. The byproduct  $\text{Li}_2\text{CO}_3$ , which forms an insulating layer as the reaction proceeds, coats on the cathode surface and suppresses the kinetics of both discharging and charging process, introducing overpotentials. The decomposition mechanism of  $\text{Li}_2\text{CO}_3$  is still under debate. Its decomposition requires a high voltage, approx. 4 V, which is close to the cutoff voltage on charge, thereby reducing the round-trip efficiency and



Deqing Cao received her B.S. degree in Chemistry from Huainan Normal University in 2017. Currently, she works as a graduate student in Nanjing Tech University and mainly engages in lithium-air battery research.



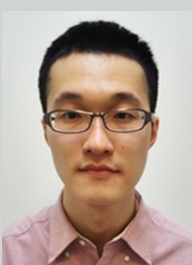
Shuaishuai Zhang received his B.S. degree in Huaibei Normal University in 2015. He is currently a Ph.D. student in Nanjing Tech University. His research is focused on the energy storage materials, e.g. super capacitors and metal air batteries.



Dr. Fengjiao Yu graduated with B.S. degree from Fudan University in 2010. After obtaining Ph.D. degree from University of St Andrews in 2014, she carried out postdoctoral work in the same university. She started research work at Nanjing Tech University in 2018 and her research focuses on the functional nanomaterials in electrocatalysis.



Prof. Yuping Wu is currently the head of School of Energy in Nanjing Tech University. He obtained his Ph.D. degree from the Institute of Chemistry of the Chinese Academy of Sciences in 1997. He has worked in Tsinghua University, Waseda University in Japan and Chemnitz University of Technology in Germany for 2 years. In 2003, he start his research in Fudan University. In 2015, he moved to Nanjing Tech University. His research interests include lithium-ion battery and its key materials, super capacitors, new energy storage system and devices, and solar hydrogen production.



Prof. Yuhui Chen obtained his Ph.D. degree from University of St Andrews in 2014. Later he worked with Prof. Peter Bruce in University of Oxford on the topic of metal-air batteries. In 2017, he joined Nanjing Tech University. His research interests include electrochemical catalysis and novel batteries such as metal air batteries.

coulombic efficiency of the Li–O<sub>2</sub> cells. Freunberger and coworkers<sup>[22]</sup> showed that the <sup>1</sup>O<sub>2</sub> was formed during the oxidation of Li<sub>2</sub>CO<sub>3</sub> and it leads to further side-reactions of electrolytes.

The decomposition of carbon should not be ignored in the Li–O<sub>2</sub> batteries. However, the carbon cannot be abandoned because it has some advantages that other materials do not own. For example, its low cost, light weight and diverse structures make it the most likely electrode material for practical use. A feasible strategy is to modify the carbon by combining with some non-carbon materials, thus the electrode possesses the superiority of carbon and the stability of non-carbon materials. These non-carbon materials also act as catalysts for the discharging and charging process. Therefore, the modified carbon materials provide more possibilities of cathodes in the Li–O<sub>2</sub> batteries.

## 2. Requirements for the Cathode

Designing an appropriate cathode electrode is a pressing issue to achieve nonaqueous Li–O<sub>2</sub> batteries with a satisfactory electrochemical performance. Three challenges are remained for the present cathodes (Figure 2):

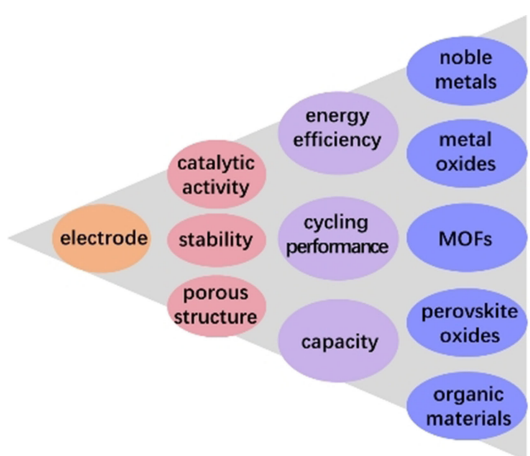


**Figure 2.** Challenges remained in the cathode of Li–O<sub>2</sub> batteries and typical carbon-free materials for cathodes of Li–O<sub>2</sub> batteries.

- (1) Poor catalytic activity towards ORR and OER, resulting in low rate of discharging and charging process.
- (2) Parasitic reactions of carbon under O<sub>2</sub>, including the decomposition itself during charging process.
- (3) Pore clogging occurs during discharging process, which impedes the mass transport of O<sub>2</sub>, intermediates and products and thus restricts the discharge capacity.

Therefore, an ideal cathode should possess at least three characteristics:

(1) Catalytic activity. Catalyst is one of the main components of cathode which plays an important role in reducing overpotential in both ORR and OER process. Both homogeneous electrocatalysts such as redox mediators and heterogeneous

electrocatalysts have been studied. The most common heterogeneous catalysts include noble metal catalysts, metal oxides, perovskite oxides, etc., which will be discussed later. It is worth to mention that reaction mechanisms vary at different electrocatalysts<sup>[23,24]</sup> and the catalytic activity is affected by many factors. Recent studies showed that different facets have different activities<sup>[23b],[25]</sup>. Generally, O<sub>2</sub> is adsorbed on the surface and then reduced, the reduced species (typically peroxide species) desorb, diffuse away and grow on the Li<sub>2</sub>O<sub>2</sub> surface. Due to the low conductivity of Li<sub>2</sub>O<sub>2</sub>, the active sites will be blocked very soon if the peroxide species fail to desorb and diffuse away rapidly.

The kinetics of ORR on carbon surface was studied and it is sufficiently fast so that kinetics of ORR seems not to be the bottleneck of the overall reaction<sup>[26]</sup>. However enormous number of studies shows that heterogeneous electrocatalyst improve the performance of batteries. No matter the electrocatalyst is required or not, at least these electrocatalysts should promote the desired reaction instead of side-reactions. Therefore, the efficacy of electrocatalysts has to be estimated carefully.<sup>[27]</sup> Electrocatalysts do reduce the overpotential and improve the reversibility of cells, particularly the columbic efficiency.<sup>[28,29,30]</sup> However, it is hard to judge whether the discharge/charge process is based on a back-to-back reversible reaction, such as formation and decomposition of Li<sub>2</sub>O<sub>2</sub>, LiO<sub>2</sub>, Li<sub>2</sub>O, etc, as the chemical yields of product were not reported in most literature. Early studies have proved that irreversible reactions in carbonate-based electrolytes could lead to the reversibility of cells<sup>[31]</sup>, but the apparent reversible cycling is based on the continuous consumption of electrolyte and accumulation of by-products. Even tens of cycles with almost 100% columbic efficiency was demonstrated,<sup>[31]</sup> it is hard to be further improved due to the irreversible chemistry. Therefore, the quantification of products and O<sub>2</sub> consumption using e.g. TiOSO<sub>4</sub> titration method<sup>[32]</sup> and online mass spectrometry should be provided together with the cycling profiles of cells.

(2) Stability. It includes the stability of material itself as well as the stability towards the intermediates (e.g. superoxide, singlet O<sub>2</sub>) and final product Li<sub>2</sub>O<sub>2</sub>. It is worth mentioning that side-reactions are inevitable and they are not always bad things. Solid electrolyte interface (SEI) formed at the anode in the Li-ion batteries is a good example. It originates from side-reactions between Li anode and electrolyte but it protects the Li anode from further side-reactions. The property of by-product is very important, it may be a good thing as long as it forms a relatively stable Li-conductive SEI layer, rather than an insulating layer like Li<sub>2</sub>CO<sub>3</sub>.

(3) A porous structure. One of the cathode functions is to serve as the mass transport channels for O<sub>2</sub>, Li<sup>+</sup> and discharge intermediate, e.g. LiO<sub>2</sub>, etc. However, it should be pointed out that the irregular deposition of Li<sub>2</sub>O<sub>2</sub> will lead to thick film and toroid particles, which cause serious pore clogging and poor cycling performance. Therefore, a cathode with sufficient void space is required and many different porous structure cathodes have been studied. The structures of catalysts strongly depend on the materials and some materials have unique structures

and morphologies. Thus, the detailed discussion of structure will be discussed in section 5.

In the text below, we summarize some recent work on the carbon-free materials for nonaqueous Li–O<sub>2</sub> cells, such as noble metals, metal oxides, MOFs, perovskite oxides and organic materials. Then we discuss the exploration on the electrodes of modified carbon. These electrodes combine the advantages of the carbon and carbon-free materials, which is a promising and feasible way for the practical Li–O<sub>2</sub> batteries. The porous structure of the electrode is crucial because the mass transport dramatically influences the electrochemical performance of the cell. The structures of these carbon-free electrodes are discussed in the section 5.

### 3. Carbon-Free Materials

The modification of carbon is a potential way to solve the problem of instability of carbon materials. To achieve this target, researchers have to explore the carbon-free materials first and understand their properties in the Li–O<sub>2</sub> cells. Before designing modified carbon cathode, the carbon-free materials possess many advantages that the carbon does not have and they introduce many possibilities of Li–O<sub>2</sub> cathode. Therefore, the studies on the nature of carbon-free materials is helpful to understand reactions itself and extend the boundary of traditional cathode materials.

#### 3.1. Noble Metals

Noble metals usually have good electrocatalytic properties and stability and thus they are often used in fundamental research. For example, Au, Pt and Ag are always applied as planar electrodes in cyclic voltammetry. Ag and Au are good substrate for some spectrometry methods, e.g. surface enhanced Raman spectrometry (SERS) and surface enhanced infrared spectrometry.<sup>[33,34,35]</sup> Single crystal electrodes of noble metals such as Pt, Au and Ir were used in studies of ORR.<sup>[36,37,38]</sup> Noble metals, including Pt, Pd, Ru, Au and their alloy are extensively studied as both ORR and OER electrocatalysts for Li–O<sub>2</sub> cells.<sup>[35,39,40]</sup>

Gold electrode has excellent chemical stability and it has certain advantages in design and synthesis. Additionally, it is

also the most ideal cathode material for reaction mechanism study of the Li–O<sub>2</sub> battery because it allows in-situ SERS experiment to identify the discharge and charge intermediates. Peng et al.<sup>[41]</sup> tested the nanoporous gold electrode in Li–O<sub>2</sub> batteries in different electrolyte systems and found that the gold electrode has good stability in the DMSO/LiClO<sub>4</sub> electrolyte system (Figure 3). As the gold electrode itself is highly chemical-stable, degradation of the Au electrode itself during cycling is minimized. It was the first time that the reversible cycle was realized (capacity maintained more than 95 % after 100 cycles). Chen and co-workers<sup>[35]</sup> studied the nanoporous gold with in-situ TEM, and revealed that high population of kinks and steps on the curved surface plays a main role for the high catalytic activities of nanoporous gold. Au and Au alloys have been used as catalysts in Li–O<sub>2</sub> batteries. Lu et al.<sup>[39]</sup> studied the noble metals Au and Pt and found that the Au catalyst can catalyze ORR effectively but the catalytic effect on OER is not obvious. In contrast, Pt showed good OER performance and its catalytic performance for ORR is not too prominent. Inspired by this, they attempted to combine Pt and Au.<sup>[42]</sup> The Pt–Au alloy catalyst effectively reduced the overpotential of both ORR and OER in the Li–O<sub>2</sub> cells. Besides Au–Pt alloy, other alloys such as Au–Ni alloy was also investigated. Kim et al.<sup>[43]</sup> used a simple electrodeposition method to prepare Ni nanowire electrode coated by Au nanoparticles without any binder or carbon. The Au–Ni composite electrode exhibited a high capacity of 591 mAhg<sup>-1</sup><sub>Au</sub> and stability of 110 cycles at current of 500 mA g<sup>-1</sup><sub>Au</sub>. An all-metal cathode system was reported by Zhang and co-workers<sup>[44]</sup> for the first time, which is an Au–Ni alloy doped on nanoporous Ni scaffold on Ni substrate. Little side-reactions towards Li<sub>2</sub>O<sub>2</sub> and LiO<sub>2</sub> were identified in this all-metal cathode system. It confirmed that the use of carbon-free materials could inhibit the decomposition of electrode. After 40 cycles, a Li<sub>2</sub>O<sub>2</sub> chemical yield of 87.7% was still remained.

Although the gold has certain advantages, its high price makes it more suitable for fundamental research. Pd is cheaper compared with Au, thus Pd was studied in Li–O<sub>2</sub> batteries. Zhang and co-workers<sup>[45]</sup> synthesized a Pd-modified integrated air electrode with a unicompartmental tunnel. The cell using the catalyst reached more than 200 cycles with limited capacity. Such stable cycling performance was attributed to Pd catalyst modified cathode that can tailor the deposition behavior as well as

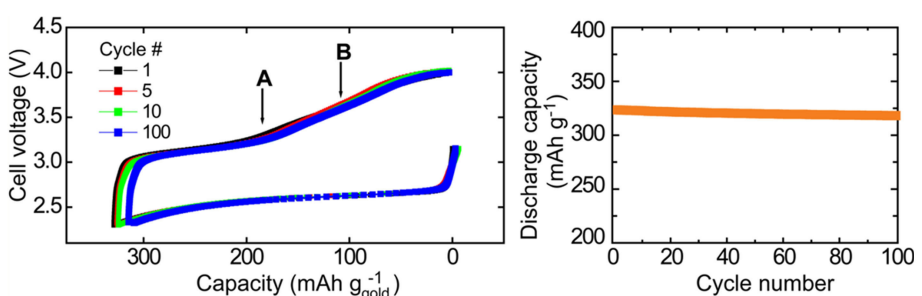


**Figure 3.** Discharge-charge profiles and cycling performance of Li–O<sub>2</sub> battery using Au nanoporous cathode. Reprinted with permission from Ref. [28]. Copyright 2012 Science.

morphology of the discharge products. Pd alters the adsorption energy of  $\text{Li}_2\text{O}_2$  and encourages the deposition of  $\text{Li}_2\text{O}_2$  along the surface of electrode substrate to form loose nanosheets rather than large  $\text{Li}_2\text{O}_2$  toroidal particles that would clog pores. This growing mode is beneficial to the deposition of reactants and reaction products. Loose holes also facilitate mass transport. Lei et al.<sup>[46]</sup> prepared carbon-loaded nano-Pd by atomic layer deposition technique as the cathode material in  $\text{Li}-\text{O}_2$  cell. The amount of Pd has a vital effect on battery performance. The material deposited with 3 layers of Pd exhibited the highest discharge specific capacity ( $6600 \text{ mAh g}^{-1}$ ), while the electrode deposited with 10 layers of Pd exhibited the lowest charging voltage (3.4 V vs.  $\text{Li}^+/\text{Li}$ ). Pd alloys were also studied. Luo et al.<sup>[47]</sup> prepared 1D porous AgPd–Pd nanotube, in which  $\text{O}_2$  and electrolyte diffusion was significantly improved. A discharge capacity up to  $2650 \text{ mAh g}^{-1}$  was obtained at  $0.2 \text{ mA cm}^{-2}$  and a round-trip efficiency up to 78% was achieved. Luo et al.<sup>[48]</sup> used pulsed laser deposition method to prepare polycrystalline Pt–Gd alloy on a Ni substrate. The battery showed improved performance and the voltage gap between discharge and charge is 1.2 V at  $0.1 \text{ mA cm}^{-2}$  even after 100 cycles.

As the cheapest noble metal among the members of the platinum group, ruthenium and its oxides have been the most extensively studied and most effective catalysts for  $\text{Li}-\text{O}_2$  batteries. Carbon supported nano-ruthenium metal particles were synthesized by Sun et al.<sup>[49]</sup> and applied as the  $\text{Li}-\text{O}_2$  battery electrode catalyst, which greatly reduced the overpotential of the battery. However, the reaction is carried out on a carbon-based electrode and reactions occurring on the surface of the carbon are always complicated. In order to eliminate the impact of the carbon electrode on the catalyst, Zhou and co-workers<sup>[50,51]</sup> applied Ru/ITO and Ru/STO as the cathode, which effectively reduce the overpotential in ORR and OER as well as amount of  $\text{Li}_2\text{CO}_3$  formation.

Although noble metals exhibit the promising catalytic performance both at discharge and charge, the high cost and heavy weight make them unattractive for the practical application in  $\text{Li}-\text{O}_2$  batteries. They are suitable for fundamental research and the results provide researcher a baseline of the electrochemical performance. Precious metals have promoted the battery performance, but more efforts can be further invested into the study on the mechanism of charge and discharge reactions.

### 3.2. Metal Oxides

The studies of metal oxides on ORR/OER has been going on for many years, especially in aqueous system and there are lots of experience to learn from. The most widely used metal oxides include Co oxides, Mn oxides, Ru oxides and Ti oxide-based materials.

#### 3.2.1. Co Oxides

$\text{Co}_3\text{O}_4$  is widely used in  $\text{Li}-\text{O}_2$  batteries due to its good catalytic performance, controllable structure and simple synthesis method. The most attention is focused on the structures and catalytic activity of  $\text{Co}_3\text{O}_4$ . Cui et al.<sup>[52]</sup> firstly prepared a free-standing  $\text{Co}_3\text{O}_4$  nanowire array mounted on the Ni foam substrate. The use of arrayed air electrodes has certain advantages. For example, the gap between the arrays provides sufficient room for cathode reaction, thus the volume effect of the electrode is well relieved during the charge and discharge process of the cell (Figure 4). However, decomposition reaction of the electrolyte is dominant because of the use of propylene carbonate-based electrolyte, which is known to react with superoxide intermediate. Therefore, the reversible profile sustained for only 5 cycles. Since the decomposition of organic carbonate-based electrolytes was raised, later work used more stable ether-based electrolytes in the  $\text{Li}-\text{O}_2$  cells. Riaz et al.<sup>[53]</sup> successfully synthesized various  $\text{Co}_3\text{O}_4$  architectures on the foamed nickel by chemical methods, including the nanosheets, nanoneedles and nanoflowers (Figure 5). They found that architecture of  $\text{Co}_3\text{O}_4$  significantly influence the specific capacity. The nanosheet architecture  $\text{Co}_3\text{O}_4$  achieved higher capacity than nanosheets and nanoflowers architecture.  $\text{Co}_3\text{O}_4$  composites was also studied. Chen et al.<sup>[54]</sup> synthesized a 3D core shell composite by incorporating the  $\text{RuO}_2$ ,  $\text{MnO}_2$  and  $\text{Co}_3\text{O}_4$  into the channels of nanoporous gold. Due to highly conductive porous structure and its great catalytic performance towards ORR and OER, it possesses much lower overpotential on both discharge and charge. Leng et al.<sup>[55]</sup> designed a flower-like  $\text{Co}_3\text{O}_4$  nanowire clusters on a Ni foam substrate and Pd nanoparticles were doped on the  $\text{Co}_3\text{O}_4$  clusters to enhance the catalytic activity.  $\text{Li}_2\text{O}_2$  grows uniformly on the electrode and the cell showed an excellent performance.

Besides, people also investigated the influence of discharge rate on the morphologies of discharge products  $\text{Li}_2\text{O}_2$  on  $\text{Co}_3\text{O}_4$  electrodes. Lee et al.<sup>[56]</sup> produced a highly catalytic cathode by

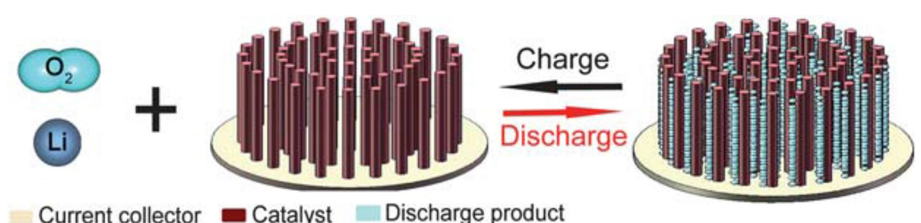
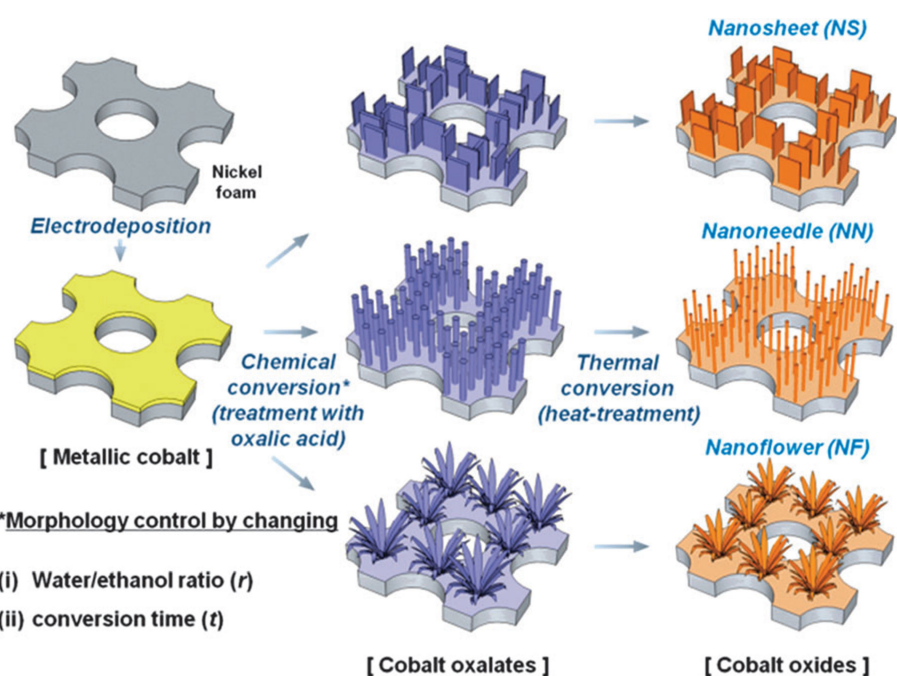


Figure 4. Free-standing  $\text{Co}_3\text{O}_4$  cathode used in  $\text{Li}-\text{O}_2$  battery. Reprinted with permission from Ref. [39]. Copyright 2011 Energy Environment Science.



**Figure 5.** Nanosheets, nanoneedles and nanoflowers  $\text{Co}_3\text{O}_4$  cathode used in  $\text{Li}-\text{O}_2$  batteries. Reprinted with permission from Ref. [40]. Copyright 2013 Chemical Communication.

growing organized  $\text{Co}_3\text{O}_4$  nanowires vertically on Ni-foam using a hydrothermal method. They found that the morphologies of discharge product are dependent on the discharge rate. Crystalline  $\text{Li}_2\text{O}_2$  is favored at a low rate, which will damage the structures of nanowire array, while amorphous  $\text{Li}_2\text{O}_2$  is favored at a high rate which covers on  $\text{Co}_3\text{O}_4$  surface evenly providing stable cycling profile. In contrast, Cao et al.<sup>[57]</sup> found that the crystalline  $\text{Li}_2\text{O}_2$  was easy to decompose on charge. They synthesized  $\text{Co}_3\text{O}_4$  nanowire on Ni foam substrate decorated with Pt nanoparticles and a low polarization of cell was observed. This catalyst encourages the formation of crystalline  $\text{Li}_2\text{O}_2$  on discharge and thus facilitates its subsequent recharging process.

In these works,  $\text{Co}_3\text{O}_4$  increases the discharge capacity and significantly reduces the charge potential. Therefore, it acts both as the electrode substrate and as the catalyst. The good catalytic activity of  $\text{Co}_3\text{O}_4$  make it a promising cathode material for  $\text{Li}-\text{O}_2$  batteries.

### 3.2.2. Mn Oxides

Mn oxide has been extensively studied for ORR in aqueous system.<sup>[58,59,60]</sup> It has a good catalytic activity like Co oxide but it is more competitive than Co oxide in price. It owns many advantages, i.e. environmental-friendly, low cost, abundant resource and etc. Therefore,  $\text{MnO}_2$  has been one of the most widely-used catalysts in the early studies of  $\text{Li}-\text{O}_2$  batteries.  $\text{MnO}_2$  improves the cycling efficiency of the battery, as well as enhances the discharge specific capacity.  $\text{MnO}_2$  was introduced as a catalyst for  $\text{Li}-\text{O}_2$  batteries by Ogasawara et al.<sup>[61]</sup> in 2006. After that, the group studied the oxides of manganese ( $\alpha$ -

$\text{MnO}_2$ ,  $\delta\text{-MnO}_2$ ,  $\gamma\text{-MnO}_2$ ,  $\lambda\text{-MnO}_2$ ) with different morphologies and structures.<sup>[31]</sup> Hu et al.<sup>[62]</sup> reported a 3D sponge-like  $\varepsilon\text{-MnO}_2$  nanostructure binder-free cathode. This electrode exhibited a high-rate capacity of  $6300 \text{ mAh g}^{-1}$  at the current density of  $500 \text{ mA g}^{-1}$  and good reversibility over 120 cycles with restricted discharge capacity. Unfortunately, all of the above tests are carried out in carbonate-based electrolytes, and they do not truly reflect the catalytic activity of  $\text{MnO}_2$ , whereas they might be worthy revisiting in future. Mn oxides has also been studied. Mn oxides can construct 3D structure and unique structure. Lin et al.<sup>[63]</sup> synthesized 3D  $(\text{Co}, \text{Mn})_3\text{O}_4$  nanowires@Ni electrode. The unique structure provides high convenience for reactants mass transport and products deposition, and undoubtedly lessens the polarization of the cell.

### 3.2.3. Ru Oxides

Ru based catalysts have good catalytic activity in OER in aqueous system. Ru oxide ( $\text{RuO}_2$ ) electrodes were first used in nonaqueous  $\text{Li}-\text{O}_2$  cells by Zhou and co-workers.<sup>[64,65,66]</sup> The overpotential on charge was significantly reduced. Jian et al.<sup>[66]</sup> used carbon nanotubes as the substrate with  $\text{RuO}_2$  layer coating on the surface. The layer of  $\text{RuO}_2$  does not only increases the specific surface area of the electrode to reduce the overpotential but also protects the carbon nanotubes (Figure 6). Although the protection on carbon tubes is not perfect, it inhibits the reaction of the carbon electrode to a certain extent and enhances the stability of the electrode. Yilmz et al.<sup>[67]</sup> explored the morphology of  $\text{Li}_2\text{O}_2$  formed on the carbon nanotubes loaded with  $\text{RuO}_2$  catalyst. They found that the addition of the  $\text{RuO}_2$  catalyst changed the morphology of  $\text{Li}_2\text{O}_2$

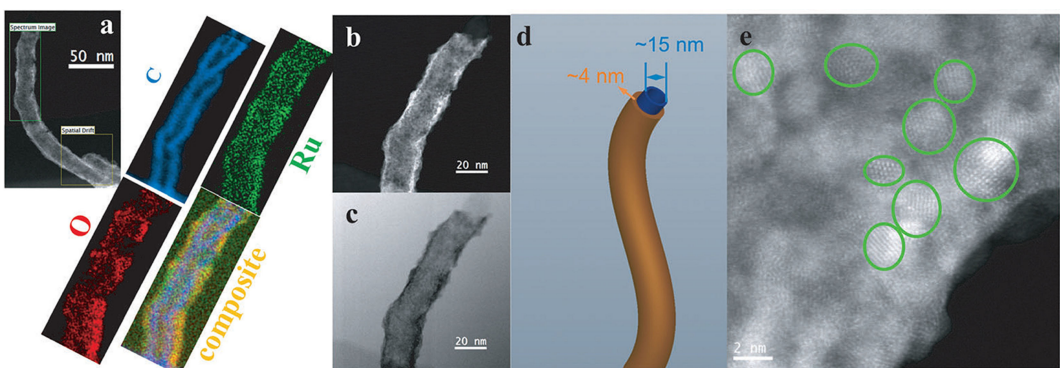


**Figure 6.** The structure of  $\text{RuO}_2$  coated on carbon nanotubes cathode. Reprinted with permission from Ref. [54]. Copyright 2014 Angewandte Chemie International Edition.

from the common toroidal shape to amorphous film. The amorphous product on carbon nanotube is more conductive and easier to be decomposed than the toroidal particles on charge.

Li et al.<sup>[64]</sup> used  $\text{RuO}_2$  hollow spheres without conductive agents as a carbon-free cathode. An overpotential of 0.13 V on discharge was obtained. Liao et al.<sup>[65]</sup> used the 2D  $\text{RuO}_2$  nanosheet as the cathode, which functions as a support as well as a bifunctional catalyst. The good conductivity ensures the low resistance during the discharge and charge process and the excellent catalytic effect contributes to the superior performance.

### 3.2.4. Ti-Based Materials

Ottakam Thotiyl et al.<sup>[68]</sup> demonstrated that TiC has a balance of conductivity and stability. The improved stability was attributed to the partially oxidized layer of  $\text{TiO}_x$  on the TiC surface. Later,  $\text{TiO}_x$  based materials have been extensively studied. Zhao et al.<sup>[69]</sup> applied the  $\text{TiO}_2$  nanotube arrays coated with Pt as cathode. Compared to carbon,  $\text{TiO}_2$  electrode itself is more stable and electrolyte TEGDME is stable on  $\text{TiO}_2$  electrode, hence a cycling performance of more than 140 cycles at high current densities is achieved. Wang et al.<sup>[70]</sup> used  $\text{TiO}_2$  with oxygen vacancies acting as the catalyst in  $\text{Li}-\text{O}_2$  cells. The oxygen vacancies at the surface promote the oxygen adsorption and dissociation and thus the cell exhibits good electrochemical performance.

Due to the poor conductivity of bulk  $\text{TiO}_2$ , a conductive Ti oxide, Magneli phase  $\text{Ti}_4\text{O}_7$ , was studied by Kundu et al.<sup>[71]</sup>. They reported the use of  $\text{Ti}_4\text{O}_7$  relieves the cathode corrosion. The advantages of high conductivity and large specific area together with the stable conductive  $\text{TiO}_{2-x}$  surface contribute to the reversible formation/decomposition of products  $\text{Li}_2\text{O}_2$ . Adam et al.<sup>[72]</sup> studied the nature of surface films on carbon and conductive Ti-based nanoparticles with various techniques. They claimed that the kinetics of  $\text{Li}_2\text{O}_2$  decomposition strongly depend on the surface conductivity and passivation.

### 3.3. MOFs and Derivatives

Metal-organic frameworks (MOFs) materials are popular catalysts for ORR. Particularly some MOF derivatives can work as single-atom catalysts.<sup>[73,74]</sup> The metal sites provide the catalytic activity by tuning the adsorption energy of  $\text{O}_2$  species. The MOFs own mesoporous structure itself, which does not only work as mass transport channels for species like electrolyte and oxygen, but also offer room for storing  $\text{Li}_2\text{O}_2$ .<sup>[75]</sup> Various MOFs were studied. Wu et al.<sup>[76]</sup> prepared the  $\text{O}_2$  cathodes based on MOF-5, HKUST-1, Mg-MOF-74, Mn-MOF-74 and Co-MOF-74. These MOFs electrodes deliver high capacities up to  $9420 \text{ mAh g}^{-1}$ , which is over 4 times higher than the capacity with merely carbon electrode. Yin et al.<sup>[77]</sup> synthesized hierarchical mesoporous  $\text{ZnO}/\text{ZnFe}_2\text{O}_4/\text{C}$  (ZZFC) nanocages. The ZZFC cathode exhibited a large specific capacity up to  $11000 \text{ mAh g}^{-1}$  at a current density of  $300 \text{ mA g}^{-1}$ . The cell presented stability for 15 cycles with a restricted capacity of  $5000 \text{ mAh g}^{-1}$ . The hierarchical structure contributes to the improved capacity.

Although MOFs have good catalytic effect and hierarchical porous structures, their restricted conductivities impede its application in cathode. They need to be combined with highly conductive carbon substrate to increase the conductivity. Recently, some MOFs with high conductivity (greater than  $5000 \text{ Sm}^{-1}$ ) have been studied, which allows their potential application as cathode materials without carbon conductor.<sup>[78,79]</sup> MOFs were also used as a template to prepare  $\text{O}_2$  cathode. Li et al.<sup>[80]</sup> demonstrated N-doped Fe-graphene cathode materials using N–Fe–MOF material with giant polyhedral cages (cage size ca. 1.8 nm) as a template.

### 3.4. Perovskites

Perovskite-type oxides were commonly used in fuel cells for ORR and they have also attracted much interest in nonaqueous  $\text{Li}-\text{O}_2$  batteries recently because they could improve the kinetics of ORR and OER. Perovskite oxides have a cubic structure and the general composition of perovskites conforms to the formula  $\text{ABO}_3$ , in which A refers to a rare-earth or alkaline-earth cation such as La, Ba, Sr, Pb, etc. and B refers to a

transition metal cation such as Mn, Ni, Co, Fe, etc. The substitution of A and B sites with other metal cations distorts the crystal structure and introduces oxygen defects and therefore enhances the catalytic performance.<sup>[81,82,83]</sup>

$\text{LaXMnO}_3$  ( $\text{X}=\text{Sr, Ba, Pb, etc.}$ ) has been extensively studied.<sup>[84,85]</sup> Xu et al.<sup>[84]</sup> firstly proposed using the electro-spinning technique combined with heating method to prepared porous  $\text{La}_{0.75}\text{Sr}_{0.25}\text{MnO}_3$  nanotubes. Although the capacity was improved, no obvious overpotential change was observed. Later, Francia et al.<sup>[85]</sup> studied the performance of  $\text{La}_{0.65}\text{X}_{0.35}\text{MnO}_3$  ( $\text{X}=\text{Ba, Sr, Pb}$ ) and found the charge overpotential is reduced by approx. 300 mV through the use of  $\text{La}_{0.65}\text{Sr}_{0.35}\text{MnO}_3$ . Wang et al.<sup>[86]</sup> substitute the Mn in  $\text{La}_{0.75}\text{Sr}_{0.25}\text{MnO}_3$  with Ni. The  $\text{La}_{0.8}\text{Sr}_{0.2}\text{Mn}_{0.6}\text{Ni}_{0.4}\text{O}_3$  reduced the overall overpotential by 180 mV and the cell achieved a discharge capacity up to  $5364 \text{ mAh g}^{-1}$ .  $\text{La}_x\text{Sr}_{1-x}\text{CoO}_3$  based perovskite oxides also exhibited good catalytic performances.<sup>[87,88,89]</sup> Fe-substituted  $\text{La}_{0.6}\text{Sr}_{0.4}\text{Co}_{0.2}\text{Fe}_{0.8}\text{O}_3$  and  $\text{Ba}_{0.9}\text{Co}_{0.7}\text{Fe}_{0.2}\text{Nb}_{0.1}\text{O}_{3-\delta}$  were shown to improve both capacity and cycleability.<sup>[90,91]</sup>  $\text{LaNiO}_3$  and derivatives were studied and they promote the oxidation of  $\text{Li}_2\text{O}_2$  and thus decrease the overpotential on charge.<sup>[92,93,94]</sup>

Perovskite oxides is a type of common catalysts for fuel cells and ORR/OER. They have a very flexible structure and flexible surface condition which can be tuned by substitutions of A/B-sites and non-stoichiometry of oxygen. Previous studies mainly were carried out in the aqueous solution instead of the non-aqueous solution. However, the reactions are different in aqueous electrolyte and nonaqueous electrolyte. Therefore, previous experiences in fuel cells cannot be simply transferred to  $\text{Li}-\text{O}_2$  cells, and the detailed electrochemical reaction mechanisms on the surface of perovskites in nonaqueous electrolyte have to be addressed properly.

### 3.5. Organic Electrode Materials

Organic electrode materials have been extensively investigated in Li-ion batteries due to their unique merits of being environmental friendly, degradable and flexible.<sup>[95,96,97,98,99,100]</sup> The flexibility of the organic electrode allows its potential application in the wearable devices. Organic electrode materials have been explored in  $\text{Li}-\text{O}_2$  batteries as well, particularly as catalysts.

Fu et al.<sup>[101]</sup> synthesized highly conductive polyaniline (PANI) membranes by proton doping method and used it as the waterproof barriers for  $\text{Li}-\text{O}_2$  batteries. The cell exhibited a specific capacity of  $3241 \text{ mAh g}^{-1}_{\text{carbon}}$  under high relative humidity ( $\text{RH} > 20\%$ ) conditions. However, a carbonate-based electrolyte was used in this work, which has been proved to be unstable and easy to decompose on discharge. Lu et al.<sup>[102]</sup> synthesized some conducting polyaniline nanofibers doped with phosphate ester. It works as catalyst for  $\text{Li}-\text{O}_2$  cells and the discharge capacity keep steady for 30 cycles with only 4% capacity loss after the initial activation process. Although the performance of cell is not satisfying, it provides a new choice for cathode materials using in rechargeable  $\text{Li}-\text{O}_2$  batteries.

Cui et al.<sup>[103]</sup> firstly introduced the polypyrrole with a tubular morphology in the  $\text{Li}-\text{O}_2$  cells. The high hydrophilicity and

conductivity of tubular polypyrrole made it a good support and the cell exhibited superior electrochemical performance. Zhang et al.<sup>[104]</sup> studied polypyrrole with different dopants as the cathode catalysts in  $\text{Li}-\text{O}_2$  cells. The polypyrrole that is doped with  $\text{Cl}^-$  exhibited enhanced discharge capacity and improved cyclability compared to the polypyrrole doped with  $\text{ClO}_4^-$ . They proposed that the formation of  $\text{LiCl}$  layer help to reduce the reaction between the electrode and electrolyte.

Poly(3,4-ethylenedioxothiophene) (PEDOT) is a type of conductive polymer electrode and it has been used in  $\text{Li}-\text{O}_2$  batteries<sup>[105,106,107]</sup>. Nasybulin et al.<sup>[105]</sup> showed that PEDOT significantly reduced the overpotential of the charging process of  $\text{Li}-\text{O}_2$  cell, due to the redox activity of PEDOT itself. Park and co-workers<sup>[106]</sup> proposed PEDOT-PSS as a multi-functional composite material for  $\text{Li}-\text{O}_2$  cells. PEDOT-PSS acts both as a redox catalyst and as a conducting binder in the air electrode. Later, they<sup>[107]</sup> synthesized the PEDOT microflowers and found these PEDOT microflowers suppress the unwanted side reaction. Mitraka et al.<sup>[108]</sup> revealed that the PEDOT electrode is electrochemically reduced (undoped) in the voltage range of ORR regime, which means it has a low conductivity. However, reacting with  $\text{O}_2$  keeps PEDOT electrode conducting, ensuring it to act as an electrode for the ORR.

Although organic electrodes have been widely studied in the metal-ion batteries, its application in  $\text{Li}-\text{O}_2$  cells needs more work. Particularly, it is a potential way to make a wearable device. Different to other non-carbon materials, there are two additional requirements of the organic cathode: conductivity & stability.

The organic polymer materials should have sufficiently high conductivity to avoid a significant resistance. Compared to inorganic materials, organic materials could be simply deposited as a thin film on surface of carbon substrate, by electrochemical methods, e.g. electro-polymerization. Therefore, the requirement of its conductivity is not strict as long as the film is sufficiently thin and does not lead to a high resistance.

Stability of the organic electrodes is not very satisfying at present, but is worthy exploring. The organic material should not decompose or react with reactants and products in the voltage range of operating potential of a  $\text{Li}-\text{O}_2$  cell, which is from 2.3 V to 3.8 V typically. Recent work did not include the chemical yield of  $\text{Li}_2\text{O}_2$  product formed on discharge, therefore it is hard to estimate its stability. However, the use of redox mediators for both discharge and charge can address the stability issue to some extent. Coupling with redox mediators, organic electrodes can potentially overcome the stability barrier.

### 4. Modified Carbon Materials

As a result of the merits of carbon, such as low cost and light weight, it is still the first choice for practical applications in the future. For the challenges of stability and catalytic activity, the modification of carbon electrode combines the advantages of carbon and carbon-free materials and thus it could make a better electrode. Here we focus on the materials which surface

are mainly covered with carbon-free materials and have the minimized carbon surface exposed to electrolyte, namely an ideal core-shell structure, rather than simple mixed carbon-catalyst composite electrodes.

Jian et al.<sup>[66]</sup> fabricated a core-shell structure RuO<sub>2</sub> catalyst by coating RuO<sub>2</sub> on the surface of carbon nanotubes. This core-shell structure effectively takes the advantage of catalytic effect of RuO<sub>2</sub> and prevents direct contact between the carbon nanotubes and Li<sub>2</sub>O<sub>2</sub>. Therefore, the formation of Li<sub>2</sub>CO<sub>3</sub> by reaction of carbon substrate and Li<sub>2</sub>O<sub>2</sub> was avoided. Yoon et al.<sup>[109]</sup> employed the polyimide coated carbon nanotubes as the electrode with the addition of a redox mediator, CsI. More than 250 cycles with a discharge capacity of 1500 mAh g<sup>-1</sup> was demonstrated. The excellent cycling performance benefits from the synergic effect of electrode and CsI. Other than coating for direct protection, some noncarbon material was grown on carbon substrate to increase the total surface area and thus reduce the ratio of carbon surface in the total electrode surface.

Liu et al.<sup>[110]</sup> employed a 3D NiCo<sub>2</sub>O<sub>4</sub> nanowire array-carbon cloth as the cathode. They observed the Li<sub>2</sub>O<sub>2</sub> porous balls deposited on the tip of NiCo<sub>2</sub>O<sub>4</sub> nanowires and those ball decomposed reversibly on the subsequent recharging process. Kwak et al.<sup>[111]</sup> presented a Mo<sub>2</sub>C nanoparticles nanostructured cathode which was found to have high coulombic efficiency (88%). Such performance is attributed to the efficient catalytic activity of Mo<sub>2</sub>C along with the MoO<sub>3</sub>-like layers on Mo<sub>2</sub>C. For comparison, the electrochemical performances of various electrode materials are listed in Table 1.

## 5. Electrode Structure

Despite the large specific surface area and porous structure of carbon, its pore structures are irregular, unless it is synthesized using specific methods like using template. Additionally, most pores are small pores (<2 nm), which has little contribution to

**Table 1.** Summary of the electrochemical performance of the various electrodes used in Li–O<sub>2</sub> batteries.

Materials	Current density [mA g <sup>-1</sup> ]	Electrolyte	Overcharge potential	Capacity [mAh g <sup>-1</sup> ]	Reference
Pt–Au nanoparticles	100	1 M LiClO <sub>4</sub> – PC:DME (1:2)	≈0.7 V (*)	≈1200	[42]
nanoporous Au	500 <sub>(Au)</sub>	0.1 M LiClO <sub>4</sub> – DMSO	≈1 V (*)	≈3000	[41]
AgPd–Pd nanotube	100	1 M LiCF <sub>3</sub> SO <sub>3</sub> – TEGDME	≈1.1 V (*)	2650	[47]
Au/Ni	500 <sub>(Au)</sub>	1.3 M LiTFSI – TEGDME	≈1 V (*)	591(Au)	[43]
Pt–Gd	0.05 mA cm <sup>-2</sup>	1M LiCF <sub>3</sub> SO <sub>3</sub> – TEGDME	≈0.7 V (*)	≈2700	[48]
Co <sub>3</sub> O <sub>4</sub>	12.5	1 M LiPF <sub>6</sub> – PC	≈0.5 V	4000	[52]
RuO <sub>2</sub> -NPG	100	1 M LiClO <sub>4</sub> – DMSO	1.05 V	300(#)	[54]
MnO <sub>2</sub> -NPG			0.96 V		
Co <sub>3</sub> O <sub>4</sub> -NPG			0.85 V		
Co <sub>3</sub> O <sub>4</sub> NW@Ni	94	1 M LiClO <sub>4</sub> – DMSO	≈1 V	4531	[56]
Pd/Co <sub>3</sub> O <sub>4</sub> /NF	60	1 M LiTFSI – TEGDME	0.8 V (*)	1842	[55]
Pt/Co <sub>3</sub> O <sub>4</sub>	100	0.1 M LiClO <sub>4</sub> – DME	1.12 V	1400	[57]
α-MnO <sub>2</sub>	70	1 M LiPF <sub>6</sub> – PC	≈1.2 V (*)	3000	[31]
(Co,Mn) <sub>3</sub> O <sub>4</sub> @Ni	0.05 mA cm <sup>-2</sup>	1 M LiTFSI – TEGDME	≈1.5 V	3605	[56]
ε-MnO <sub>2</sub>	500	1 M LiTFSI – TEGDME	≈1.2 V (*)	6300	[62]
CNT@RuO <sub>2</sub>	100	LiTFSI – Triglyme	0.51 V	3258	[66]
2D RuO <sub>2</sub> nanosheet	200	1 M LiClO <sub>4</sub> – DMSO	0.59 V	900	[65]
Pt/TiO <sub>2</sub>	1000(Pt)	1 M LiTFSI – TEGDME	≈0.6 V (*)	1000(#)	[69]
Ti <sub>4</sub> O <sub>7</sub>	12.5	0.5 M LiTFSI – TEGDME	≈0.5 V	≈350	[71]
TiC	500	0.5 M LiClO <sub>4</sub> – DMSO	≈1 V	500	[68]
MOF-5	50	1 M LiTFSI – TEGDME	–	1780	[76]
HKUST-1				4170	
Mg-MOF-74				4560	
Mn-MOF-74				9420	
Co-MOF-74				3630	
ZnO/ZnFe <sub>2</sub> O <sub>4</sub> /C	300	1 M LiTFSI – TEGDME	≈1 V	11000	[77]
Fe–N-MOF	50	1 M LiPF <sub>6</sub> – TEGDME	0.79 V	5300	[80]
La <sub>0.75</sub> Sr <sub>0.25</sub> MnO <sub>3</sub>	25	1 M LiTFSI – TEGDME	≈1 V	≈10000	[84]
La <sub>0.8</sub> Sr <sub>0.2</sub> Mn <sub>0.6</sub> Ni <sub>0.4</sub> O <sub>3</sub>	200	1 M LiCF <sub>3</sub> SO <sub>3</sub> – TEGDME	–	500(#)	[86]
La <sub>0.65</sub> Pb <sub>0.35</sub> MnO <sub>3</sub>	200	0.5 M LiClO <sub>4</sub> – TEGDME	≈1.3 V (*)	7211	[85]
LaNiO <sub>3</sub>	267	1 M LiCF <sub>3</sub> SO <sub>3</sub> – TEGDME	≈1 V (*)	500(#)	[92]
La <sub>0.6</sub> Sr <sub>0.4</sub> Co <sub>0.2</sub> Fe <sub>0.8</sub> O <sub>3</sub>	200	1 M LiTFSI – DMSO	0.91 V	13979	[90]
Polyaniline Nanofibers	0.05 mA cm <sup>-2</sup>	1 M LiBF <sub>4</sub> – PC	≈1.3 V (*)	3260	[102]
Polyaniline membrane	0.1 mA cm <sup>-2</sup>	1 M LiPF <sub>6</sub> – PC/DMC	–	3241	[101]
Tubular polypyrrole	0.1 mA cm <sup>-1</sup>	LiTFSI – DME	≈0.8 V (*)	1982	[103]
Doped polypyrrole	50	0.1MLiTFSI – DME	≈0.8 V (*)	2626	[104]
PEDOT	0.1 mA cm <sup>-2</sup>	1 M LiTFSI – TEGDME	–	1900	[105]
PEDOT microflowers	20	0.5 M LiTFSI/0.5 M LiNO <sub>3</sub> – TEGDME	≈1.3 V	≈1200	[107]
PEDOT:PSS	400	1 M LiTFSI – TEGDME	≈1.4 V (*)	1000(#)	[106]
polyimide-coated carbon	500	1 M LiTFSI – TEGDME	0.62 V	1,500(#)	[109]
RuO <sub>2</sub> @CNT	100	LiTFSI – Triglyme	≈0.7 V (*)	3258	[66]
NiCo <sub>2</sub> O <sub>4</sub>	18	1 M LiTFSI – DME	≈1 V	1000(#)	[110]
Mo <sub>2</sub> C	200	1 M LiCFSO <sub>3</sub> – TEGDME	≈0.5 V	1000(#)	[111]

\* represents the approximate value estimated from the original data, # represents limited capacity.

capacity due to the difficulty of access. A porous structure with interconnected and thorough holes is ideal for the air electrodes in a Li–O<sub>2</sub> cell. Some materials such as metal oxide and MOFs are easier to construct a better porous structure and gas channels, and thus the cells deliver a high capacity and good rate capability. Several novel cathode structures have been used in Li–O<sub>2</sub> cells in the past few years.

When designing a new structure for Li–O<sub>2</sub> cathode, whether it possesses a relative high surface area that would provide more active sites is the first criterion to consider. The high surface area typically leads to low true current density and low overpotential thus less surface route, which reduce surface passivation. Much work has been done following this guideline. For example, Nazar and co-workers<sup>[112]</sup> used a chemical precipitation method to synthesize nanocrystalline lead ruthenium oxides (PbRO) and bismuth ruthenium oxides (BiRO) composite electrode with an unique expanded pyrochlore structure. Gold nanoparticle is deposited on the electrode surface function as the catalyst for ORR. The performances of both ORR and OER process are improved due to the good catalytic activity of gold and increased active sites offered by high surface of the unique structure composite electrode respectivelt. Riaz et al.<sup>[113]</sup> fabricated a cathode of new structure, which comprised of one-dimensional NiCo<sub>2</sub>O<sub>4</sub> nanoneedle arrays with a thin MnO<sub>2</sub> nanoflake coating (Figure 7a). The cell delivered a good performance with the capacity up to 2372 mAh g<sup>-1</sup> and low charge overpotential owing to the high porosity and large surface of the electrode. Yoon et al. constructed a similar structure.<sup>[114]</sup> They synthesized a brush-like Co<sub>4</sub>N nanorods, which were anchored on N-doped carbon paper (Figure 7b). The discharge capacity of Li–O<sub>2</sub> cell with this electrode is as high as 11.9 mAh cm<sup>-2</sup> areal, which is several times higher than the typical areal specific capacity of a commercial Li-ion cell (3–5 mAh cm<sup>-2</sup> areal). The structure improves the charge transfer and provides numerous active sites.

The pore size in porous structure for Li–O<sub>2</sub> battery is also a crucial factor. The mesopores offer active sites, the macropores offer mass transport channel. Zhang et al.<sup>[115]</sup> prepared a mesoporous (usually refers to size at the range of 2–50 nm) Co<sub>3</sub>Mo<sub>3</sub>N electrode that offers numerous active sites. The well-designed electrode delivered an excellent electrocatalytic performance. Wang et al.<sup>[116]</sup> synthesized spinel mesoporous CuCo<sub>2</sub>O<sub>4</sub> that possessed higher ORR and OER activities and the cell exhibits enhanced electrochemical performances with a high capacity of 5288 mAh g<sup>-1</sup>. Zhao et al.<sup>[117]</sup> developed a hierarchical porous Co<sub>3</sub>O<sub>4</sub> films with size-adjustable mesopores and kinetics of O<sub>2</sub> diffusion varied according to the pore size (Figure 7d). A capacity of 2460 mAh g<sup>-1</sup> was achieved with the film catalyst, and more than 35 cycles was remained with a limited capacity of 1000 mAh g<sup>-1</sup>.

The property of the cathode material itself plays a significant role as well as the large surface area does. Lin et al.<sup>[118]</sup> firstly reported an open-structured Co<sub>9</sub>S<sub>8</sub> matrix with sisal morphology (Figure 7c). The high affinity to oxygen of Co<sub>9</sub>S<sub>8</sub> plays a key role in enhanced performance of the cell. The cell shows an enhanced capacity of 6875 mAh g<sup>-1</sup> and a charge overpotential of 0.57 V.

## 6. Outlook

In summary, there are lots of choices for carbon-free materials. Exploring new materials is crucial to further development of the Li–O<sub>2</sub> batteries. Carbon-free electrodes are of many unique merits compared with carbon-based electrodes and it can work as both electrode substrate and catalysts. The study of pure carbon-free materials allows us understand the materials itself better therefore it is definitely worth more efforts. Some material such as perovskite oxides has been extensively investigated in aqueous systems, but the reactions on their

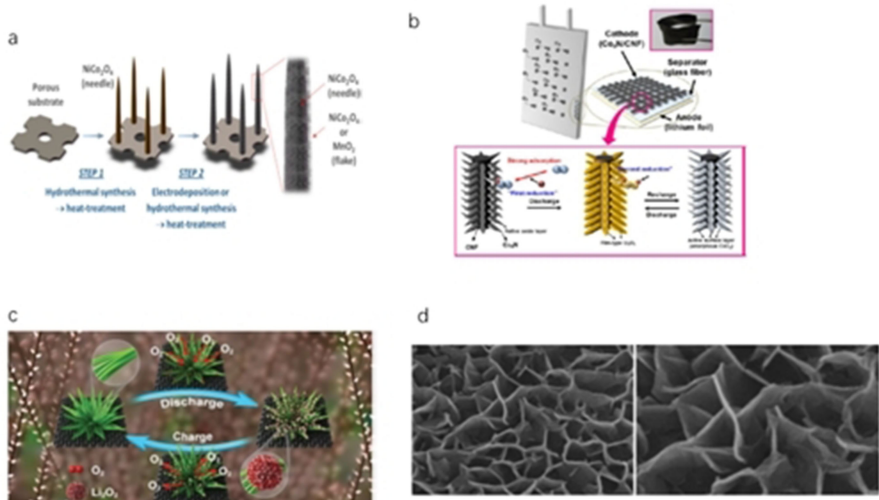


**Figure 7.** Schematics of four typical structures of the porous electrode in Li–O<sub>2</sub> batteries: a) 1-D nanoneedle arrays decorated with nanoflakes. Reprinted with permission from Ref. [101]. Copyright 2014 ACS applied materials & interfaces. b) brush-like metallic Co<sub>4</sub>N nanorods. Reprinted with permission from Ref. [102]. Copyright 2018 ACS Nano. c) Open-structured Co<sub>9</sub>S<sub>8</sub> matrix with sisal morphology. Reprinted with permission from Ref. [106]. Copyright 2018 Advance Energy Material. d) Hierarchical porous Co<sub>3</sub>O<sub>4</sub> film. Reprinted with permission from Ref. [105]. Copyright 2013 The Journal of Physical Chemistry C.

surface in the nonaqueous electrolytes could be completely different. Therefore, these catalysts should be revisited in the nonaqueous systems rather than simply transferring from the aqueous systems. Due to the heavy weight of carbon-free materials, the most feasible approach is to combine the advantages of carbon and carbon-free to make best use of them. The modified materials are expected to overcome the problems of traditional carbon materials. Although recently defected graphene structure and graphene with N-doped exhibited catalytic activity for ORR and OER in aqueous solution, the defects on the carbon surface might be attacked by the reactive reduced oxygen species like superoxide and cause more carbon decomposition, leading to an even worse stability. However, these surface defects could be beneficial as long as they help to immobilize the catalysts coating on the carbon surface. More studies are required in nonaqueous electrolyte to address this issue.

## Acknowledgements

Y.C. is indebted to 1000 Youth Talents Plan of National Natural Science Foundation of China (grant number 51773092) and Research Fundation of State Key Lab (ZK201717).

## Conflict of Interest

The authors declare no conflict of interest.

**Keywords:** carbon-free materials • cathode materials • energy storage • Li–O<sub>2</sub> batteries • metal oxides

- [1] K.-N. Jung, J. Kim, Y. Yamauchi, M.-S. Park, J.-W. Lee, J. H. Kim, *J. Mater. Chem. A* **2016**, *4*, 14050–14068.
- [2] C. Ling, R. Zhang, K. Takechi, F. Mizuno, *J. Phys. Chem. C* **2014**, *118*, 26591–26598.
- [3] F. Li, S. Wu, D. Li, T. Zhang, P. He, A. Yamada, H. Zhou, *Nat. Commun.* **2015**, *6*, 7843.
- [4] K. M. Abraham\*, Z. Jiang, *J. Electrochem. Soc.* **1996**, *143*, 1–5.
- [5] E. L. Littauer\*, K. C. Tsai\*, *J. Electrochem. Soc.* **1976**, *123*, 771–776.
- [6] A. Kraysberg, Y. Ein-Eli, *J. Power Sources* **2011**, *196*, 886–893.
- [7] a) K. W. Semkow, A. F. Sammeils, *J. Electrochem. Soc.* **1987**, *134*, 2084–2085.; b) B. Kumar, J. Kumar, R. Leese, J. P. Fellner, S. J. Rodrigues, K. M. Abraham, *J. Electrochem. Soc.* **2010**, *157*, A50.
- [8] Y. Wang, H. Zhou, *J. Power Sources* **2010**, *195*, 358–361.
- [9] Y. Wang, P. He, H. Zhou, *Energy Environ. Sci.* **2011**, *4*, 4994.
- [10] V. Giordani, D. Tozier, H. Tan, C. M. Burke, B. M. Gallant, J. Uddin, J. R. Greer, B. D. McCloskey, G. V. Chase, D. Addison, *J. Am. Chem. Soc.* **2016**, *138*, 2656–2663.
- [11] C. Xia, C. Y. Kwok, L. F. Nazar, *Science* **2018**, *361*, 777–781.
- [12] Tao Liu, Michal Leskes, Wanjing Yu, Amy J. Moore, Lina Zhou, Paul M. Bayley, Gunwoo Kim, C. P. Grey, *Science* **2015**, *350*, 530–533.
- [13] J. Lu, Y. J. Lee, X. Luo, K. C. Lau, M. Asadi, H. H. Wang, S. Brombosz, J. Wen, D. Zhai, Z. Chen, D. J. Miller, Y. S. Jeong, J. B. Park, Z. Z. Fang, B. Kumar, A. Salehi-Khojin, Y. K. Sun, L. A. Curtiss, K. Amine, *Nature* **2016**, *529*, 377–382.
- [14] B. D. McCloskey, A. Speidel, R. Scheffler, D. C. Miller, V. Viswanathan, J. S. Hummelshøj, J. K. Norskov, A. C. Luntz, *J. Phys. Chem. Lett.* **2012**, *3*, 997–1001.
- [15] J. Huang, Z. Peng, *Batteries & Supercaps* **2019**, *2*, 37–48; *Supercaps* **2019**, *2*, 37–48.
- [16] B. M. Gallant, R. R. Mitchell, D. G. Kwabi, J. Zhou, L. Zuin, C. V. Thompson, Y. Shao-Horn, *J. Phys. Chem. C* **2012**, *116*, 20800–20805.
- [17] R. R. Mitchell, B. M. Gallant, C. V. Thompson, Y. Shao-Horn, *Energy Environ. Sci.* **2011**, *4*, 2952.
- [18] W. Xu, J. Hu, M. H. Engelhard, S. A. Towne, J. S. Hardy, J. Xiao, J. Feng, M. Y. Hu, J. Zhang, F. Ding, M. E. Gross, J.-G. Zhang, *J. Power Sources* **2012**, *215*, 240–247.
- [19] M. M. Ottakam Thotiyil, S. A. Freunberger, Z. Peng, P. G. Bruce, *J. Am. Chem. Soc.* **2013**, *135*, 494–500.
- [20] T. K. Zakharchenko, A. Y. Kozmenkova, D. M. Itkis, E. A. Goodilin, *Beilstein J. Nanotechnol.* **2013**, *4*, 758–762.
- [21] a) L. Schafzahl, N. Mahne, B. Schafzahl, M. Wilkening, C. Slugovc, S. M. Borisov, S. A. Freunberger, *Angew. Chem. Int. Ed.* **2017**, *56*, 15728–15732; *Angew. Chem.* **2017**, *129*, 15934–15938; b) Nika Mahne, Bettina Schafzahl, Christian Leybold, M. Leybold, S. Grumm, A. Leitgeb, G. A. Strohmeier, M. Wilkening, O. Fontaine, D. Kramer, C. Slugovc, S. M. Borisov, S. A. Freunberger, *Nat. Energy* **2017**, *2*, 17036.
- [22] Nika Mahne, S. E. Renfrew, B. D. McCloskey, S. A. Freunberger, *Angew. Chem. Int. Ed.* **2018**, *57*, 5529–5533; *Angew. Chem.* **2018**, *130*, 5627–5631.
- [23] a) J. S. Hummelshøj, A. C. Luntz, J. K. Nørskov, *J. Chem. Phys.* **2013**, *138*; b) N.-C. Lai, G. Cong, Z. Liang, Y.-C. Lu, *Joule* **2018**, *2*.
- [24] Yu Wang, Z. Lian, Q. Zou, G. Cong, Y.-C. Lu, *J. Phys. Chem. C* **2016**, *120*, 6459–6466.
- [25] J. Zhu, X. Ren, J. Liu, W. Zhang, Z. Wen, *ACS Catal.* **2015**, *5*, 73–81.
- [26] B. D. McCloskey, R. Scheffler, A. Speidel, G. Girishkumar, A. C. Luntz, *J. Phys. Chem. C* **2012**, *116*, 23897–23905.
- [27] B. D. McCloskey, R. Scheffler, A. Speidel, D. S. Bethune, R. M. Shelby, A. C. Luntz, *J. Am. Chem. Soc.* **2011**, *133*, 18038–18041.
- [28] Raymond A. Wong, Chunzhen Yang, A. Dutta, M. O. M. Hong, M. L. Thomas, K. Yamanaka, T. Ohta, K. Waki, H. R. Byon, *ACS Energy Lett.* **2018**, *3*, 592–597.
- [29] N. Mahne, O. Fontaine, M. O. Thotiyil, M. Wilkening, S. A. Freunberger, *Chem. Sci.* **2017**, *8*, 6716–6729.
- [30] B. D. McCloskey, D. Addison, *ACS Catal.* **2017**, *7*, 772–778.
- [31] A. Débart, A. J. Paterson, J. Bao, P. G. Bruce, *Angew. Chem. Int. Ed.* **2008**, *120*, 4597–4600.
- [32] B. D. McCloskey, A. Valery, A. C. Luntz, S. R. Gowda, G. M. Wallraff, J. M. Garcia, T. Mori, L. E. Krupp, *J. Phys. Chem. Lett.* **2013**, *4*, 2989–2993.
- [33] K. Kneipp, A. S. Haka, H. Kneipp, K. Badizadegan, N. Yoshizawa, C. Boone, Karen E. Shafer-Peltier, J. T. Motz, R. R. Dasari, M. S. Feld, *Appl. Spectrosc.* **2002**, *56*, 150–154.
- [34] H. Miyake, S. Ye, M. Osawa, *Electrochem. Commun.* **2002**, *4*, 973–977.
- [35] T. Fujita, P. Guan, K. McKenna, X. Lang, A. Hirata, L. Zhang, T. Tokunaga, S. Arai, Y. Yamamoto, N. Tanaka, Y. Ishikawa, N. Asao, Y. Yamamoto, J. Erlebacher, M. Chen, *Nat. Mater.* **2012**, *11*, 775–780.
- [36] P. P. Lopes, D. Strmcnik, J. S. Jirkovsky, J. G. Connell, V. Stamenkovic, N. Markovic, *Catal. Today* **2016**, *262*, 41–47.
- [37] V. Stamenkovic, B. S. Mun, K. J. J. Mayrhofer, P. N. Ross, N. M. Markovic, J. Rossmeisl, J. Greeley, J. K. Nørskov, *Angew. Chem. Int. Ed.* **2006**, *118*, 2963–2967.
- [38] J. Greeley, I. E. Stephens, A. S. Bondarenko, T. P. Johansson, H. A. Hansen, T. F. Jaramillo, J. Rossmeisl, I. Chorkendorff, J. K. Nørskov, *Nat. Chem.* **2009**, *1*, 552–556.
- [39] Y.-C. Lu, H. A. Gasteiger, M. C. Parent, V. Chiloyan, Y. Shao-Horn, *Electrochem. Solid-State Lett.* **2010**, *13*, A69.
- [40] Y. C. Lu, H. A. Gasteiger, Y. Shao-Horn, *J. Am. Chem. Soc.* **2011**, *133*, 19048–19051.
- [41] Z. Peng, S. A. Freunberger, Y. Chen, P. G. Bruce, *Science* **2012**, *337*, 563–566.
- [42] Y.-C. Lu, Z. Xu, H. A. Gasteiger, S. Chen, K. Hamad-Schifferli, Y. Shao-Horn, *J. Am. Chem. Soc.* **2010**, *132*, 12170–12171.
- [43] S. T. Kim, N.-S. Choi, S. Park, J. Cho, *Adv. Energy Mater.* **2015**, *5*, 1401030.
- [44] J. J. Xu, Z. W. Chang, Y. B. Yin, X. B. Zhang, *ACS Cent. Sci.* **2017**, *3*, 598–604.
- [45] J. J. Xu, Z. L. Wang, D. Xu, L. L. Zhang, X. B. Zhang, *Nat. Commun.* **2013**, *4*, 2438.
- [46] Y. Lei, J. Lu, X. Luo, T. Wu, P. Du, X. Zhang, Y. Ren, J. Wen, D. J. Miller, J. T. Miller, Y. K. Sun, J. W. Elam, K. Amine, *Nano Lett.* **2013**, *13*, 4182–4189.
- [47] W. B. Luo, X. W. Gao, S. L. Chou, J. Z. Wang, H. K. Liu, *Adv. Mater.* **2015**, *27*, 6862–6869.
- [48] W. B. Luo, X. W. Gao, D. Q. Shi, S. L. Chou, J. Z. Wang, H. K. Liu, *Small* **2016**, *12*, 3031–3038.

- [49] B. Sun, P. Munroe, G. Wang, *Sci. Rep.* **2013**, *3*, 2247.
- [50] F. Li, D.-M. Tang, Z. Jian, D. Liu, D. Golberg, A. Yamada, H. Zhou, *Adv. Mater.* **2014**, *26*, 4659–4664.
- [51] F. Li, D. M. Tang, Y. Chen, D. Golberg, H. Kitaura, T. Zhang, A. Yamada, H. Zhou, *Nano Lett.* **2013**, *13*, 4702–4707.
- [52] Y. Cui, Z. Wen, Y. Liu, *Energy Environ. Sci.* **2011**, *4*, 4727.
- [53] A. Riaz, K. N. Jung, W. Chang, S. B. Lee, T. H. Lim, S. J. Park, R. H. Song, S. Yoon, K. H. Shin, J. W. Lee, *Chem. Commun.* **2013**, *49*, 5984–5986.
- [54] L. Y. Chen, X. W. Guo, J. H. Han, P. Liu, X. D. Xu, A. Hirataa, M. W. Chen, *Mater. Chem.* **2015**, *3*, 3620–3626.
- [55] L. Leng, X. Zeng, H. Song, T. Shu, H. Wang, S. Liao, *J. Mater. Chem. A* **2015**, *3*, 15626–15632.
- [56] H. Lee, Y.-J. Kim, D. J. Lee, J. Song, Y. M. Lee, H.-T. Kim, J.-K. Park, *J. Mater. Chem. A* **2014**, *2*, 11891.
- [57] J. Cao, S. Liu, J. Xie, Shichao Zhang, G. Cao, X. Zhao, *ACS Catal.* **2015**, *5*, 241–245.
- [58] L. Mao, T. Sotomura, K. Nakatsu, N. Koshiba, D. Zhang, T. Ohsaka, *J. Am. Chem. Soc.* **2002**, *124*, A504.
- [59] L. Mao, *Electrochim. Acta* **2003**, *48*, 1015–1021.
- [60] Y. L. Cao, H. X. Yang, X. P. Ai, L. F. Xiao, *J. Electroanal. Chem.* **2003**, *557*, 127–134.
- [61] T. Ogasawara, A. I. D. Bart, M. Holzapfel, Petr Novák, P. G. Bruce, *J. Am. Chem. Soc.* **2006**, *128*, 1390–1393.
- [62] X. Hu, X. Han, Y. Hu, F. Cheng, J. Chen, *Nanoscale* **2014**, *6*, 3522–3525.
- [63] X. Lin, Y. Shang, T. Huang, A. Yu, *Nanoscale* **2014**, *6*, 9043.
- [64] F. Li, D.-M. Tang, T. Zhang, K. Liao, P. He, D. Golberg, A. Yamada, H. Zhou, *Adv. Energy Mater.* **2015**, *5*, 1500294.
- [65] K. Liao, X. Wang, Y. Sun, D. Tang, M. Han, P. He, X. Jiang, T. Zhang, H. Zhou, *Energy Environ. Sci.* **2015**, *8*, 1992–1997.
- [66] Z. Jian, P. Liu, F. Li, P. He, X. Guo, M. Chen, H. Zhou, *Angew. Chem. Int. Ed.* **2014**, *53*, 442–446; *Angew. Chem.* **2014**, *126*, 452–456.
- [67] E. Yilmaz, C. Yogi, K. Yamanaka, T. Ohta, H. R. Byon, *Nano Lett.* **2013**, *13*, 4679–4684.
- [68] M. M. Ottakam Thotiyil, S. A. Freunberger, Z. Peng, Y. Chen, Z. Liu, P. G. Bruce, *Nat. Mater.* **2013**, *12*, 1050–1056.
- [69] G. Zhao, R. Mo, B. Wang, L. Zhang, K. Sun, *Chem. Mater.* **2014**, *26*, 2551–2556.
- [70] F. Wang, H. Li, Q. Wu, J. Fang, Y. Huang, C. Yin, Y. Xu, Z. Luo, *Electrochim. Acta* **2016**, *202*, 1–7.
- [71] D. Kundu, R. Black, E. J. Berg, L. F. Nazar, *Energy Environ. Sci.* **2015**, *8*, 1292–1298.
- [72] Brian D. Adams, Robert Black, Claudio Radtke, Zack Williams, B. L. Mehdi, Nigel D. Browning, Linda F. Nazar, *ACS Nano* **2014**, *8*, 12483–12493.
- [73] T. Yildirim, M. R. Hartman, *Phys. Rev. Lett.* **2005**, *95*, 215504.
- [74] X. Wang, J. Zhou, H. Fu, W. Li, X. Fan, G. Xin, J. Zheng, X. Li, *J. Mater. Chem. A* **2014**, *2*, 14064–14070.
- [75] B. Y. Xia, Y. Yan, N. Li, H. B. Wu, X. W. Lou, X. Wang, *Nat. Energy* **2016**, *1*, 15006.
- [76] D. Wu, Z. Guo, X. Yin, Q. Pang, B. Tu, L. Zhang, Y. G. Wang, Q. Li, *Adv. Mater.* **2014**, *26*, 3258–3262.
- [77] W. Yin, Y. Shen, F. Zou, X. Hu, B. Chi, Y. Huang, *ACS Appl. Mater. Interfaces* **2015**, *7*, 4947–4954.
- [78] D. Sheberla, L. Sun, M. A. Blood-Forsythe, S. Er, C. R. Wade, C. K. Brozek, A. Aspuru-Guzik, M. Dinca, *J. Am. Chem. Soc.* **2014**, *136*, 8859–8862.
- [79] D. Sheberla, J. C. Bachman, J. S. Elias, C. J. Sun, Y. Shao-Horn, M. Dinca, *Nat. Mater.* **2017**, *16*, 220–224.
- [80] Q. Li, P. Xu, W. Gao, S. Ma, G. Zhang, R. Cao, J. Cho, H. L. Wang, G. Wu, *Adv. Mater.* **2014**, *26*, 1378–1386.
- [81] a) H. M. Zhang, Y. Shimizu, Y. Teraoka, N. Miura, N. Yamazoe, *J. Catal.* **1990**, *121*, 432–440; b) P. Tan, M. Liu, Z. Shao, M. Ni, *Adv. Energy Mater.* **2017**, *7*, 1–23.
- [82] S. M. Haile, G. Staneff, K. H. Ryu, *J. Mater. Sci.* **2001**, *36*.
- [83] H. Tanakaa, M. Misonob, *Curr. Opin. Solid State Mater. Sci.* **2001**, *5*, 381–387.
- [84] J. J. Xu, D. Xu, Z. L. Wang, H. G. Wang, L. L. Zhang, X. B. Zhang, *Angew. Chem. Int. Ed.* **2013**, *52*, 3887–3890; *Angew. Chem.* **2013**, *125*, 3979–3982.
- [85] C. Francia, J. Amici, E. Tasarkuyu, A. Çoşkun, Ö. F. Gü, T. Şener, *Int. J. Hydrogen Energy* **2016**, *41*, 20583–20591.
- [86] Z. Wang, Y. You, J. Yuan, Y. X. Yin, Y. T. Li, S. Xin, D. Zhang, *ACS Appl. Mater. Interfaces* **2016**, *8*, 6520–6528.
- [87] P. Li, J. Zhang, Q. Yu, J. Qiao, Z. Wang, D. Rooney, W. Sun, K. Sun, *Electrochim. Acta* **2015**, *165*, 78–84.
- [88] J. J. Lee, M. Y. Oh, K. S. Nahm, *J. Am. Chem. Soc.* **2015**, *137*, A244–A250.
- [89] N. Sun, H. Liu, Z. Yu, Z. Zheng, C. Shao, *RSC Adv.* **2016**, *6*, 13522–13530.
- [90] J. Cheng, M. Zhang, Y. Jiang, L. Zou, Y. Gong, B. Chi, J. Pu, L. Jian, *Electrochim. Acta* **2016**, *191*, 106–115.
- [91] Q. Xua, S. Song, Y. Zhang, Y. Wang, J. Zhang, Y. Ruana, M. Hand, *Electrochim. Acta* **2016**, *191*, 577–585.
- [92] J. Zhang, Y. Zhao, X. Zhao, Z. Liu, W. Chen, *Sci. Rep.* **2014**, *4*, 6005.
- [93] Q. Xu, X. Han, F. D. b, L. Zhang, L. Sang, X. Liu, Q. Xu, *J. Alloys Compd.* **2016**, *664*, 750–755.
- [94] R. S. Kalubarme, G.-E. Park, K.-N. Jung, K.-H. Shin, W.-H. Ryu, C.-J. Parka, *J. Am. Chem. Soc.* **2014**, *136*, A880–A889.
- [95] M. Armand, S. Grueon, H. Vezin, S. Laruelle, P. Ribiere, P. Poizot, J. M. Tarascon, *Nat. Mater.* **2009**, *8*, 120–125.
- [96] M. Lee, J. Hong, J. Lopez, Y. Sun, D. Feng, K. Lim, W. C. Chueh, M. F. Toney, Y. Cui, Z. Bao, *Nat. Energy* **2017**, *2*, 861–868.
- [97] C. Peng, G.-H. Ning, J. Su, G. Zhong, W. Tang, B. Tian, C. Su, D. Yu, L. Zu, J. Yang, M.-F. Ng, Y.-S. Hu, Y. Yang, M. Armand, K. P. Loh, *Nat. Energy* **2017**, *2*, 17074.
- [98] Q. C. Liu, J. J. Xu, D. Xu, X. B. Zhang, *Nat. Commun.* **2015**, *6*, 7892.
- [99] X. Y. Yang, J. J. Xu, D. Bao, Z. W. Chang, D. P. Liu, Y. Zhang, X. B. Zhang, *Adv. Mater.* **2017**, *29*.
- [100] L. Wang, Y. Zhang, J. Pan, H. Peng, *J. Mater. Chem. A* **2016**, *4*, 13419–13424.
- [101] Z. Fu, Z. Wei, X. Lin, T. Huang, A. Yu, *Electrochim. Acta* **2012**, *78*, 195–199.
- [102] Qi Lu, Qiang Zhao, Hongming Zhang, J. Li, X. Wang, F. Wang, *ACS Macro Lett.* **2013**, *2*, 92–95.
- [103] Y. Cui, Z. Wen, X. Liang, Y. Lu, J. Jin, M. Wu, X. Wu, *Energy Environ. Sci.* **2012**, *5*, 7893.
- [104] J. Zhang, B. Sun, H.-J. Ahn, C. Wang, G. Wang, *Mater. Res. Bull.* **2013**, *48*, 4979–4983.
- [105] E. Nasybulin, W. Xu, M. H. Engelhard, X. S. Li, M. Gu, D. Hu, J.-G. Zhang, *Electrochim. Commun.* **2013**, *29*, 63–66.
- [106] D. H. Yoon, S. H. Yoon, K. S. Ryu, Y. J. Park, *Sci. Rep.* **2016**, *6*, 19962.
- [107] S. H. Yoon, Y. J. Park, *RSC Adv.* **2017**, *7*, 56752–56759.
- [108] E. Mitraka, M. J. Jafari, M. Vagin, X. Liu, M. Fahlman, T. Ederth, M. Berggren, M. P. Jonsson, X. Crispin, *J. Mater. Chem. A* **2017**, *5*, 4404–4412.
- [109] S. H. Yoon, Y. J. Park, *Sci. Rep.* **2017**, *7*, 42617.
- [110] W. M. Liu, T. T. Gao, Y. Yang, Q. Sun, Z. W. Fu, *Phys. Chem. Chem. Phys.* **2013**, *15*, 15806–15810.
- [111] W.-J. Kwak, K. C. Lau, C.-D. Shin, K. Amine, L. A. Curtiss, Y.-K. Sun, *ACS Nano* **2015**, *9*, 4129–4137.
- [112] S. H. Oh, L. F. Nazar, *Adv. Energy Mater.* **2012**, *2*, 903–910.
- [113] A. Riaz, Kyu-Nam Jung, Wonyoung Chang, K.-H. Shin, J.-W. Lee, *ACS Appl. Mater. Interfaces* **2014**, *6*, 17815–17822.
- [114] K. R. Yoon, K. Shin, J. Park, S. H. Cho, C. Kim, J. W. Jung, J. Y. Cheong, H. R. Byon, H. M. Lee, I. D. Kim, *ACS Nano* **2018**, *12*, 128–139.
- [115] K. Zhang, L. Zhang, X. Chen, X. He, X. Wang, Shanmu Dong, P. Han, Chuanjian Zhang, Shan Wang, L. Gu, G. Cui, *J. Phys. Chem. C* **2013**, *117*, 858–865.
- [116] P.-X. Wang, L. Shao, N.-Q. Zhang, K.-N. Sun, *J. Power Sources* **2016**, *325*, 506–512.
- [117] G. Zhao, Z. Xu, K. Sun, *J. Mater. Chem. A* **2013**, *1*, 12862.
- [118] X. Lin, R. Yuan, S. Cai, Y. Jiang, J. Lei, S.-G. Liu, Q.-H. Wu, H.-G. Liao, M. Zheng, Q. Dong, *Adv. Energy Mater.* **2018**, *8*, 1800089.

Manuscript received: December 2, 2018

Revised manuscript received: February 3, 2019

Accepted manuscript online: February 6, 2019

Version of record online: February 21, 2019